# BASIC AND TRANSLATIONAL—LIVER

CPEB4 Increases Expression of PFKFB3 to Induce Glycolysis and Activate Mouse and Human Hepatic Stellate Cells, Promoting Liver Fibrosis

Marc Mejias,[1,2] Javier Gallego,[1,2] Salvador Naranjo-Suarez,[1] Marta Ramirez,[1] Nuria Pell,[1] Anna Manzano,[3] Clara Suñer,[4] Ramon Bartrons,[3] Raul Mendez,[4,5] and Mercedes Fernandez[1,2]

[1]Angiogenesis in Liver Disease Research Group, August Pi i Sunyer Biomedical Research Institute, Hospital Clinic, University of Barcelona, Barcelona, Spain; [2]Biomedical Research Networking Center on Hepatic and Digestive Disease, Institute of Health Carlos III, Spain; [3]Department of Physiological Sciences, University of Barcelona, Bellvitge Biomedical Research Institute, Barcelona, Spain; [4]Institute for Research in Biomedicine, The Barcelona Institute of Science and Technology, Barcelona, Spain; and [5]Institució Catalana de Recerca i Estudis Avançats, Barcelona, Spain

Gastroenterology
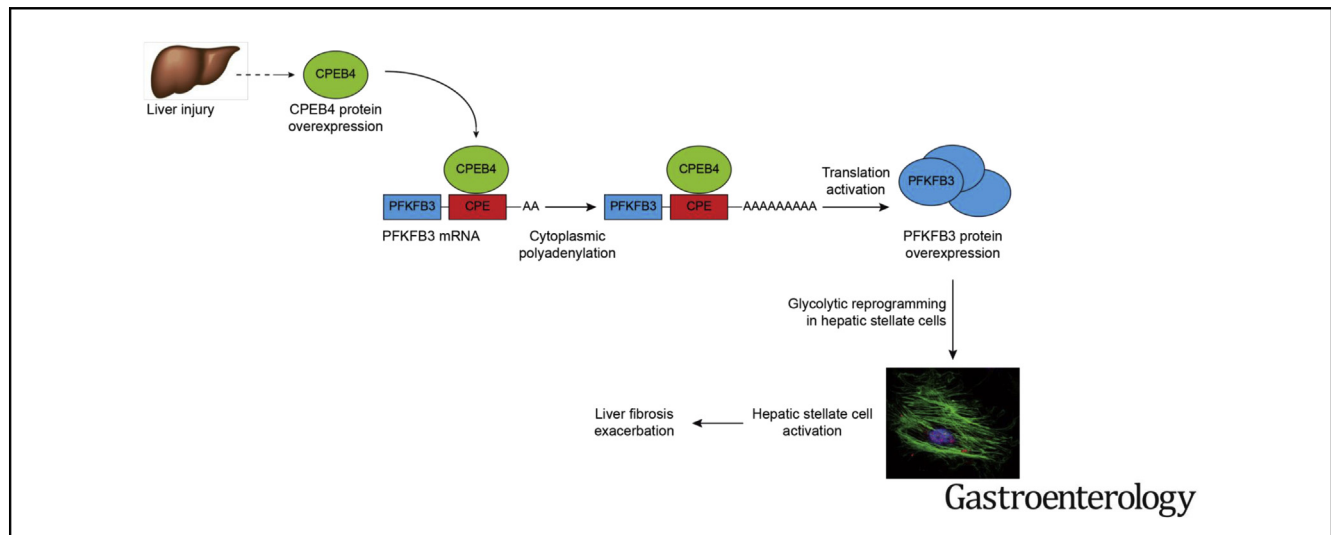
BACKGROUND & AIMS: We investigated mechanisms of hepatic stellate cell (HSC) activation, which contributes to liver fibrogenesis. We aimed to determine whether activated HSCs increase glycolysis, which is regulated by 6-phosphofructo-2-kinase/fructose-2,6-bisphosphatase-3 (PFKFB3), and whether this pathway might serve as a therapeutic target. **METHODS:** We performed studies with primary mouse HSCs, human LX2 HSCs, human cirrhotic liver tissues, rats and mice with liver fibrosis (due to bile duct ligation [BDL] or administration of carbon tetrachloride), and CPEB4-knockout mice. Glycolysis was inhibited in cells and mice by administration of a small molecule antagonist of PFKFB3 (3-[3-pyridinyl]-1-[4-pyridinyl]-2-propen-1-one [3PO]). Cells were transfected with small interfering RNAs that knock down PFKFB3 or CPEB4. **RESULTS:** Up-regulation of PFKFB3 protein and increased glycolysis were early and sustained events during HSC activation and accompanied by increased expression of markers of fibrogenesis; incubation of HSCs with 3PO or knockdown of PFKFB3 reduced their activation and proliferation. Mice with liver fibrosis after BDL had increased hepatic PFKFB3; injection of 3PO immediately after the surgery prevented HSC activation and reduced the severity of liver fibrosis compared with mice given vehicle. Levels of PFKFB3 protein were increased in fibrotic liver tissues from patients compared with non-fibrotic liver. Up-regulation of PFKFB3 in activated HSCs did not occur via increased transcription, but instead via binding of CPEB4 to cytoplasmic polyadenylation elements within the 3'-untranslated regions of PFKFB3 messenger RNA. Knockdown of CPEB4 in LX2 HSCs prevented PFKFB3 overexpression and cell activation. Livers from CPEB4-knockout had decreased PFKFB3 and fibrosis after BDL or administration of carbon tetrachloride compared with wild-type mice. **CONCLUSIONS:** Fibrotic liver tissues from patients and rodents (mice and rats) have increased levels of PFKFB3 and glycolysis, which are essential for activation of HSCs. Increased expression of PFKFB3 is mediated by binding of CPEB4 to its untranslated messenger RNA. Inhibition or knockdown of CPEB4 or PFKFB3 prevents HSC activation and fibrogenesis in livers of mice.

C hronic liver diseases are highly prevalent and associated with a high and dramatically increased burden worldwide.[1] Despite that, development of new therapeutics remains stagnant. Liver transplantation currently represents the only chance of long-term survival for patients with chronic liver disease, but the availability of appropriate donor tissue is limited, and the procedure is very expensive, necessitating a search for alternatives.

Upon liver injury, activation and transdifferentiation of hepatic stellate cells (HSCs) into scar-forming myofibroblasts is among the first responses detectable at the site of damage.[2] These cells drive a wound-healing response that relies on the deposition of collagen-rich extracellular matrix to maintain tissue integrity. This transient response must be tightly controlled, as it otherwise becomes persistent and leads to excessive matrix accumulation and fibrosis. This is what happens when facing excessive cellular stress, such as in chronic liver injury. Exacerbated fibrosis impairs normal liver function and acts as a precursor to cirrhosis, eventually leading to liver failure and death.[3,4] Understanding the molecular bases of HSC activation is therefore essential to define novel and more efficient targets of antifibrotic therapy to reduce incidence and morbidity and mortality of the people suffering from chronic liver disease.

The myofibroblastic phenotype of activated HSCs is characterized by increased proliferation and matrix production and secretion.[4] To cope with these highly energetically demanding processes, it is reasonable to assume that activated HSCs can exhibit augmented aerobic glycolysis as an additional bioenergetic and biosynthetic supply, even in oxygen-rich conditions, similarly to the observed in many cancer cells,[5–7] and other non-malignant proliferating cells.[8–10] In this regard, previous studies have appreciated the relationship among aerobic glycolysis (conversion of glucose to lactate), glutaminolysis (conversion of glutamine to α-ketoglutarate), and fibrogenesis.[11,12] Deciphering the molecular mechanisms underpinning the metabolic reprogramming in HSCs can reveal potential targets suitable for therapeutic intervention. A major driver of glycolysis is 6-phosphofructo-2-kinase/fructose-2,6-bisphosphatase-3 (PFKFB3),[13] which produces fructose-2,6-bisphosphate (F2,6BP), the most potent allosteric activator of the glycolytic rate-limiting enzyme phosphofructokinase-1 (PFK1).[14] Therefore, we investigated the impact of PFKFB3 on the activation and fibrogenic behavior of HSCs, the molecular mechanisms behind this process, and the potential utility of targeting this enzyme as a new antifibrotic strategy.

Materials and Methods

A detailed description of the Materials and Methods can be found in the Supplementary Material.

WHAT YOU NEED TO KNOW

BACKGROUND AND CONTEXT

Little is known about mechanisms of hepatic stellate cell (HSC) activation, which contributes to liver fibrogenesis.

NEW FINDINGS

Fibrotic liver tissues from patients and mice have increased levels of PFKFB3, which promotes glycolysis, and activation of HSCs. Increased expression of PFKFB3 is mediated by binding of CPEB4 to its untranslated mRNA. Inhibition or knockdown of CPEB4 or PFKFB3 prevents HSC activation and fibrogenesis in livers of mice.

LIMITATIONS

This study was performed using human cells and tissues and mice. Further studies are needed in humans.

IMPACT

Strategies to inhibit glycolysis pathways, by targeting the CPEB4-PFKFB3 circuit, in activated HSCs might be developed for treatment or prevention of liver fibrosis.

Primary Mouse Hepatic Stellate Cell Isolation and Culture

Mouse HSCs were isolated from adult BALB/c mice by retrograde pronase-collagenase liver perfusion and density centrifugation.[15] Perfusion through inferior vena cava was initiated with 15 mL of 190 mg/L EGTA solution. Portal vein was cut and vena cava clamped above the diaphragm to ensure correct liver perfusion. Then, perfusion continued with 25 mL of 0.4 mg/mL pronase solution and, finally, 35 mL of 0.1 U/mL collagenase solution. The liver was removed, minced, and incubated (10–20 minutes, 40°C, under agitation) in pronase/collagenase solution containing 1% (vol/vol) DNase. The resulting dispersed cell suspension was filtered through 70-μm cell strainer and centrifuged ($50g$, 5 minutes). HSCs were separated by Histodenz density gradient centrifugation (Sigma, St Louis, MO) and culture-activated on 12-well Nunc plates (Thermo-Fisher, Waltham, MA) or 18-mm coverslips in Dulbecco's modified Eagle medium containing 10% fetal bovine serum, 100 U/mL penicillin, 100 μg/mL streptomycin, and 2 mM L-glutamine.

Human Hepatic Stellate Cell Line and Culture

LX2 human HSC line (Merck, Madrid, Spain; SCC064) was generated by immortalization of primary human HSCs with the

SV40 large T antigen.[16] LX2 cells were cultured in high-glucose Dulbecco's modified Eagle medium containing 10% fetal bovine serum, 100 U/mL penicillin, 100 μg/mL streptomycin, and 2 mM L-glutamine.

Measurement of Fructose-2,6-Bisphosphate

Intracellular F2,6BP content was measured in LX2 cells using the Van Schaftingen's method.[17] LX2 cells were cultured for 3 days on a medium containing 7.5 μM 3PO or vehicle (dimethyl sulfoxide [DMSO]). Then, LX2 cells were homogenized in extraction buffer containing 0.1 M NaOH and 0.1% Triton X-100. The resulting mixture was heated for 5 minutes at 80°C. After cooling, cells were centrifuged and supernatant neutralized with a solution containing 10 mM HEPES in acetic acid. The mixture was centrifuged and F2,6BP content measured in the supernatant using a coupled enzyme reaction.[17]

Statistical Analysis

Data are shown as mean ± SEM. Results that were normally distributed ($P > .05$ from Kolmogorov-Smirnov test) were compared with parametric statistical procedures (Student t test and analysis of variance followed by Bonferroni test for multiple comparisons). Non-normally distributed results were compared with nonparametric tests (Kruskal-Wallis 1-way analysis of variance and Mann-Whitney U test). Significance was accepted at $P < .05$.

Results

The Protein Expression of the Key Glycolytic Enzyme PFKFB3 Is Up-Regulated During Hepatic Stellate Cell Activation

The study began characterizing the expression pattern of the critical glycolytic enzyme PFKFB3 during the activation of HSCs, the principle cells responsible for liver fibrosis. To this end, we utilized freshly isolated mouse primary HSCs undergoing culture-induced activation and transdifferentiation from a quiescent to a myofibroblastic phenotype (Figure 1A). We found that PFKFB3 expression rapidly switched on during the myofibroblastic differentiation, within 24 hours after plating, as demonstrated by co-immunofluorescence with the typical myofibroblastic marker alpha-smooth muscle actin (αSMA) (Figure 1B). These results were confirmed in the human LX2 HSC line (Figure 1A), which has been extensively characterized and retains key features of human activated HSCs.[16] We cultured LX2 cells for up to 7 days on plastic surfaces of cell culture dishes as a surrogate for the molecular changes that occur during HSCs in the injured liver. We comparatively analyzed the expression of PFKFB3 and the myofibroblastic markers αSMA , platelet-derived growth factor (PDGF), PDGF receptor-β, and collagen type I at different times by immunoblot analysis. We found that PFKFB3 protein up-regulation was an early and sustained event during HSC activation that was accompanied by increased expression of fibrogenic markers (Figure 1C). These findings support the idea that HSCs undergo a PFKFB3-regulated glycolytic reprogramming during cell activation.

PFKFB3 Blockade Attenuates Glycolysis in Hepatic Stellate Cells

To determine the biological consequences of the enhanced glycolysis, we studied the effects of the small molecule inhibitor of PFKFB3, 3-(3-pyridinyl)-1-(4-pyridinyl)-2-propen-1-one (3PO),[18] on HSCs (Figure 1D). LX2 cells were plated for 3 days on a medium containing a low dose of 3PO or vehicle (DMSO). Inhibition of PFKFB3 enzymatic activity in LX2 cells resulted in a significant 51% reduction in F2,6BP (the product of the reaction catalyzed by PFKFB3 and an allosteric activator of PFK1 and surrogate marker for the glycolytic rate) (Figure 1D), without causing cell death, in agreement with previous studies using 3PO in other cell types.[19]

PFKFB3 Blockade Reduces Hepatic Stellate Cell Activation and Profibrogenic Phenotype In Vitro

Next, we evaluated the effects of inhibition of PFKFB3-driven glycolysis on primary mouse HSCs. We found that morphological changes typically associated with HSC differentiation were blocked by the glycolytic blocker 3PO (Figure 1E). Thus, at 2 hours, before any treatment, there was a homogeneous population of cells containing lipid droplets. Within 1 day of seeding, primary mouse HSCs treated with vehicle adhered and began to put out fine cellular processes on the tissue culture plastic surface, as shown by phase-contrast light microscopy (Figure 1E). After 4 days, cells became larger and more myofibroblast-like in their appearance, with long cytoplasmic processes branching out from the stellate cell body and an expanded and flattened shape (Figure 1E). These activated HSCs also progressively lost their cytoplasmic lipid droplets (Figure 1E, refringent vesicles; and Figure 1F, Oil Red-O staining), which serve in quiescent cells as a storage compartment for vitamin A. Notably, 3PO treatment prevented the culture-induced activation of primary mouse HSCs, such that the phenotypic appearance of treated cells closely resembled that of freshly isolated quiescent cells, with a rounded morphology and abundant lipid droplets (Figure 1E and F). In addition, the typical positivity for the contractile protein αSMA, a reliable marker of the phenotypic transformation of HSCs into myofibroblast-like cells, was markedly decreased in 3PO-treated cells, both at messenger RNA (mRNA) (Figure 1G; reverse transcription polymerase chain reaction) and protein levels (Figure 1H; immunofluorescence), compared with vehicle-treated cells.

To further interrogate our results, we studied human LX2 cells. After 1, 3, or 6 days in culture, LX2 cells were exposed to low concentrations of 3PO or vehicle (DMSO) and then harvested 3 days later. We found that 3PO markedly reduced expression of core proteins in HSC activation and fibrogenesis, including αSMA, PDGF, its receptor PDGFR-β, and vascular endothelial growth factor, as assessed by immunoblotting (Figure 2A). The

overexpression of PFKFB3 observed with time in LX2 cells was also down-regulated by 3PO (Figure 2A), reflecting the decrease in glycolysis caused by the PFKFB3 blocker. Similar results were also observed in primary mouse HSCs,

as demonstrated by immunofluorescence (Figure 2B), suggesting that the antifibrotic properties of PFKFB3 inhibition are likely conserved across mammalian species. Inhibition of PFKFB3-driven glycolysis also influenced the proliferative
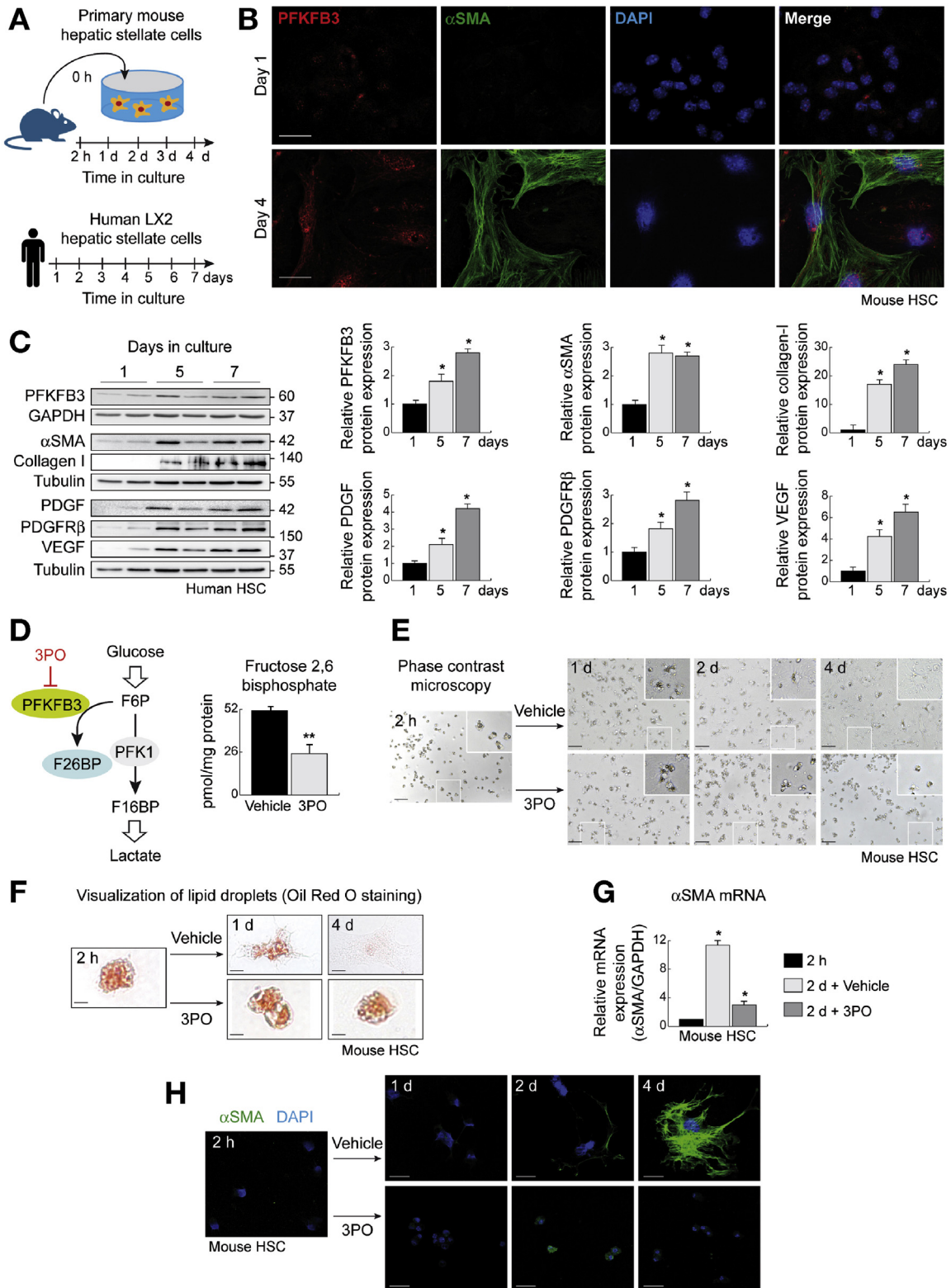
capacity of HSCs, supporting the well-established concept that glycolytic reprogramming leads to a metabolic state ideal for the proliferation and sustenance of rapidly multiplying cells.[20–22] Thus, 3PO dose-dependently reduced the rate of cell proliferation observed upon culture activation, as demonstrated by measuring the incorporation of 5'-bromo-2'-deoxyuridine to the DNA of LX2 cells by flow cytometry (Figure 2C–E), and counting cell number (Figure 2F). These results together indicate that HSCs rely heavily on PFKFB3-dependent glycolytic reprogramming to fuel cell activation, proliferation, and fibrogenesis.

To further confirm the findings with 3PO, we applied a different strategy to decrease PFKFB3 activity using small interfering RNAs (siRNA) specifically silencing the PFKFB3 gene. Human LX2 cells were incubated for 3 days (a time point at which cells are well activated and PFKFB3 protein is significantly overexpressed) (Figure 2A), and then transfected with PFKFB3 siRNAs or control siRNAs. Assays were conducted 24 or 96 hours later (Figure 2G). We found that only when PFKFB3 protein expression was efficiently reduced (at 96 hours post-transfection), the expression of αSMA protein was also effectively down-regulated (Figure 2H), further demonstrating the essential requirement of PFKFB3 up-regulation for initiation and perpetuation of the activated HSC phenotype.

PFKFB3 Protein Expression Is Elevated in Fibrotic Human and Rodent Livers

To further underscore the importance of PFKFB3 as regulator of liver fibrosis, we investigated its level of expression in human liver. We found that the expression of PFKFB3 protein was higher in the liver from patients with hepatitis C virus–related cirrhosis than in healthy tissue, as demonstrated by immunoblotting (Figure 3A) and by immunohistochemistry (Figure 3B). We next analyzed the expression profile of PFKFB3 protein in a well-established experimental model in rodents, where fibrosis is produced by bile duct ligation (BDL). Immunoblot analysis using livers from BDL rats at different time points after fibrosis induction (days 1, 3, 7, 14, and 28), and from sham-operated control rats, demonstrated gradual increase in PFKFB3 protein expression levels after BDL compared with normal livers (Figure 3C). Of note, this PFKFB3 up-regulation was observed in the nucleus as well as in the cytoplasm (Figure 3C), further suggesting a possible translocation of PFKFB3 to the nuclei to regulate cell cycle and activate cell proliferation (Figure 2C–F). Nuclear PFKFB3 expression was also detected in mouse HSC by immunofluorescence (Figures 1B and 2B). Studies in mouse fibrotic livers further confirmed these findings (Figure 3D). In both rats and mice, the overexpression of PFKFB3 protein accompanied the increase of αSMA and other markers of HSC activation, such as PDGFR-β and vascular endothelial growth factor (Figures 3C and D). These results were substantiated by co-immunofluorescence (Figure 3E) and immunohistochemistry (Figure 3F) showing that cells with spindle morphology, staining positive for both PFKFB3 and αSMA, accumulated in fibrotic livers surrounding portal tracts. These results suggest that, as in the in vitro model systems, changes in the glycolytic enzyme PFKFB3 are linked with the outgrowth of activated HSC during liver fibrosis in vivo. These spindle cells were positive for the marker of cell replication Ki67, implicating that they were proliferating (Figure 3G). This is expected because it is well known that, although in physiological conditions HSCs are mitotically quiescent, they undergo rapid and dramatic increase in proliferation after BDL.[4]

To find out more about the spatiotemporal expression pattern of PFKFB3 and its relationship with the time course of HSC activation and fibrogenesis in the fibrotic liver, we performed immunohistochemistry for PFKFB3 and αSMA, and histological staining with Sirius Red (ie, fibrosis detection) in consecutive liver sections from sham-operated control mice or mice subjected to BDL and studied at different time points thereafter. Although PFKFB3 was poorly expressed in sham animals, we found it to be abundant in portal tracts after fibrosis induction, correlating with αSMA expression and Sirius Red staining (Figure 4A). Because tissue hypoxia is a common theme in the pathways leading to PFKFB3 induction and fibrosis progression,[2,23,24] we also asked whether PFKFB3 up-regulation in liver fibrosis correlates with hypoxic areas in vivo. Using the hypoxia marker pimonidazole hydrochloride (hypoxyprobe), which is reductively activated and covalently bound to macromolecules in cells at low oxygen concentration,[24] we detected the typical oxygen gradient of the normal liver, running from central vein toward portal triads, following the normal intrahepatic blood flow (Figure 4B). Upon fibrosis induction, there was a progressive increase in

BASIC AND TRANSLATIONAL LIVER

Figure 1. PFKFB3 protein expression is up-regulated during HSC transdifferentiation, and PFKFB3 blockade attenuates glycolysis in HSCs. (A) In vitro studies were conducted in HSCs freshly isolated from mice, and in the human LX2 stellate cell line. (B) Co-immunofluorescence for PFKFB3 (*red*) and αSMA (*green*) in primary mouse HSCs cultured for 1 and 4 days. 4,6-Diamidino-2-phenylindole–stained nuclei (DAPI) (*blue*). Scale bar: 25 μm. (C) Immunoblotting and protein expression quantification for the indicated proteins in LX2 cells. (D) Schematic representation of the glycolytic pathway. PFKFB3 converts the glycolytic intermediate fructose-6-phosphate (F6P) into F2,6BP, which, in turn, enhances the activity of the rate-limiting enzyme PFK1, thereby accelerating glycolysis. The inhibitor of PFKFB3 enzymatic activity 3PO (7.5 μm) reduces F2,6BP content in LX2 cells compared with vehicle-treated cells (DMSO). (E) Phase-contrast *micrographs* of mouse HSCs after 2 hours in culture, before any treatment, and also cultured for 1, 2, and 4 days in presence or absence of 3PO (15 μm). Scale bar: 50 μm. (F) Visualization of lipid droplets by Oil Red-O staining in control and 15 μM 3PO-treated mouse HSCs. (G) αSMA mRNA expression in control and 15 μM 3PO-treated mouse HSCs. (H) αSMA immunocytofluorescence (*green*) in control and 15 μM 3PO-treated mouse HSCs. DAPI-stained nuclei (*blue*). Scale bar: 25 μm. *P < .05; **P < .01.
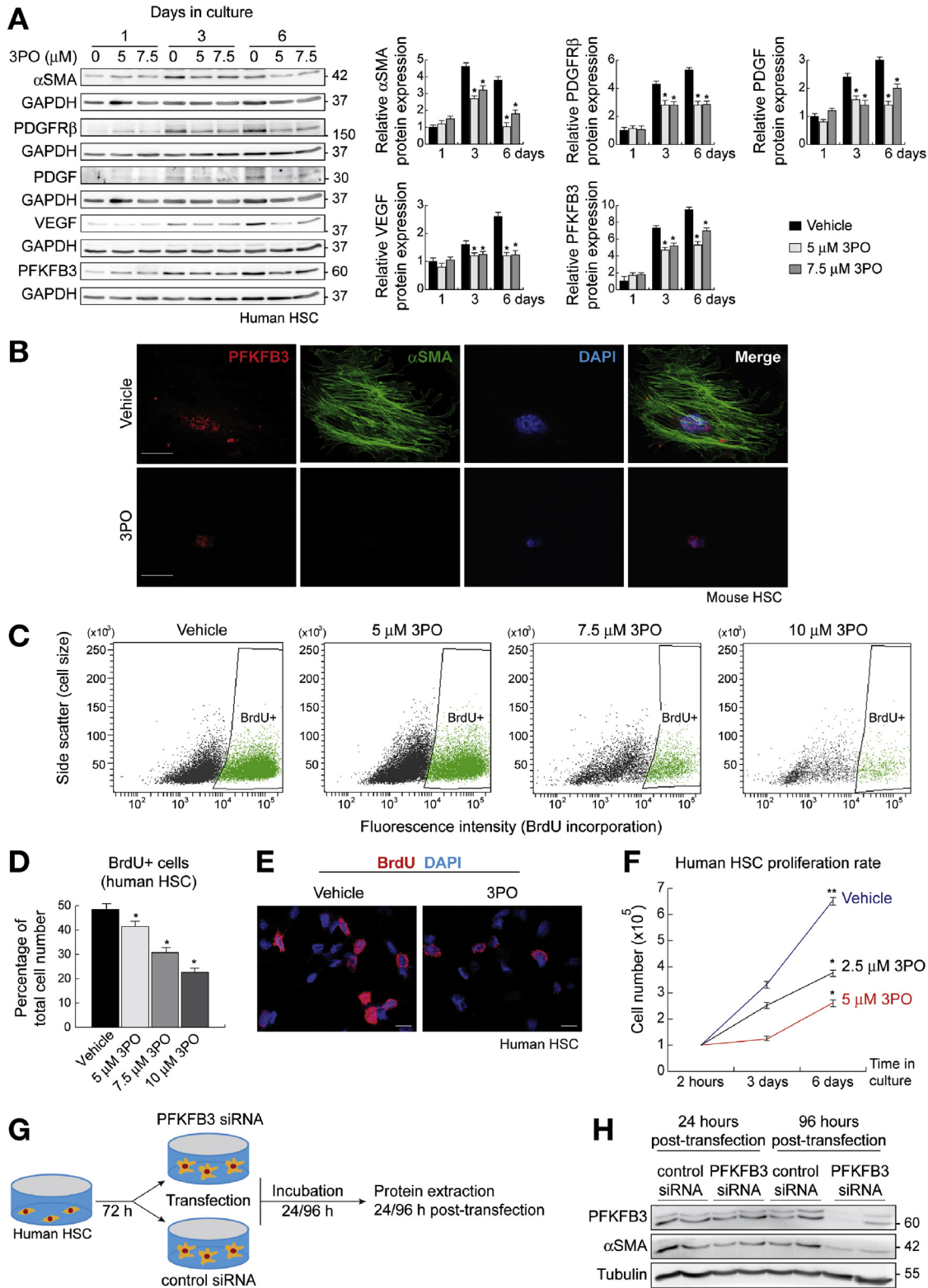
Figure 2. PFKFB3 blockade represses HSC activation and profibrogenic phenotype in vitro. (*A*) Immunoblotting and protein expression quantification for the indicated proteins in control and 3PO-treated LX2 cells. Data are mean ± SEM of 2–3 different experiments. (*B*) Co-immunocytofluorescence for PFKFB3 (*red*) and αSMA (*green*) in control or 3PO-treated mouse HSCs. 4,6-diamidino-2-phenylindole (DAPI)–stained nuclei (*blue*). Scale bar: 25 μm. (*C*) LX2 cellular proliferation measured by flow cytometric 5'-bromo-2'-deoxyuridine (BrdU) incorporation analysis. (*D*) Quantification of BrdU plots. (*E*) BrdU immunofluorescence (*red*) in control and 3PO-treated LX2 cells. DAPI-stained nuclei (*blue*). Scale bar: 25 μm. (*F*) Time course of LX2 cell proliferation in presence of 3PO or vehicle. *$P < .05$. (*G*) Schematic overview of the transfection experiment. (*H*) Immunoblotting for PFKFB3 and αSMA in LX2 cells, cultured for 72 hours, and then transfected with PFKFB3 siRNAs or control siRNAs. Assays conducted at 24 and 96 hours post-transfection.

the size of hepatocellular hypoxic areas (Figure 4B), compatible with the occurrence of liver blood supply impairment and impaired oxygen delivery to hepatocytes during fibrosis.[24] It is interesting that PFKFB3-positive cells accumulated preferentially in regions of the fibrotic liver exposed to high levels of oxygen or at least normoxic conditions (ie, portal tracts), where pimonidazole immunolabeling was almost not detectable, and less in the more
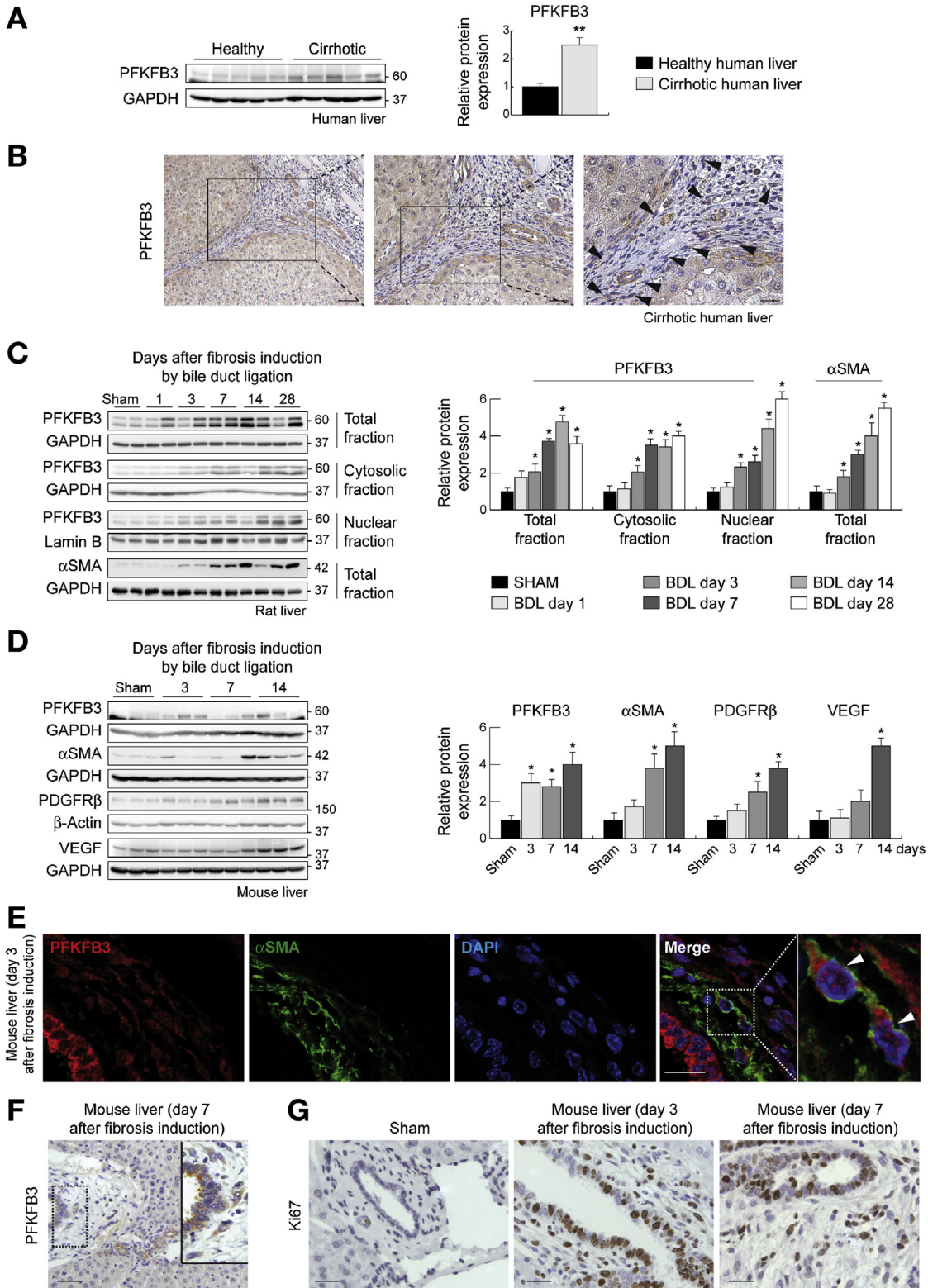
hypoxic microenvironment surrounding hepatic central veins (Figure 4B). This nonoverlapping expression pattern of pimonidazole and PFKFB3 supports that activated HSCs exhibit an abnormally high glycolytic rate regardless of the presence of adequate oxygen and is consistent with the possibility that PFKFB3 overexpression in the fibrotic liver does not require a locally hypoxic milieu for success.

PFKFB3 Blockade Reduces Fibrogenesis In Vivo

To analyze the impact of targeting PFKFB3-mediated glycolysis on HSC activation and fibrogenesis in vivo, we used mice with BDL-induced liver fibrosis, in which hepatic PFKFB3 expression is up-regulated, as demonstrated in this study (Figures 3D–F and 4A). Starting immediately after the initial surgery, the mice were administered either vehicle (DMSO) or a low dose of 3PO (35 mg/kg, intraperitoneal) (Figure 4C). There were no significant differences in body weight (Figure 4D), liver weight (Figure 4E), spleen weight (Figure 4F), or any apparent adverse side effect in BDL mice receiving 3PO compared to those treated with DMSO alone. Interestingly, pharmacological PFKFB3 inhibition by 3PO markedly prevented the activation of HSCs and the extent of fibrosis after liver damage, compared with vehicle-treated BDL mice, as indicated by counting the number of cells positive for the HSC marker desmin (Figure 4G), immuno-histochemistry for desmin (Figure 4H), and morphometric analysis of Sirius Red staining (Figures 4I and J). Because PFKFB3 overexpression after BDL was not restricted to HSCs, but also extended to biliary epithelial cells (Figures 3E and 3F), we determined the effects of PFKFB3 inhibition on ductular proliferation. Similar numbers of bile ducts were identified on H&E-stained sections from 3PO- and vehicle-treated BDL mice (Figures 4I and 4K). Taken together, these results underscore the importance of HSC glycolysis in controlling the fibrogenic process and support the potential utility of 3PO as a novel antifibrotic agent.

The Cytoplasmic Polyadenylation Element Binding Protein CPEB4 Is Functionally Linked With PFKFB3 During Hepatic Stellate Cell Activation

Understanding the molecular mechanisms responsible for the pathological induction of PFKFB3 during HSC activation can provide new therapeutic strategies for liver fibrosis. Interestingly, the progressive up-regulation of PFKFB3 during HSC activation observed on protein level by

immunofluorescence (Figure 1B) and immunoblotting (Figure 1C) was not confirmed on mRNA level, as measured by reverse transcription polymerase chain reaction (Figures 5A–C). These results indicate that the over-expression process does not require de novo transcription of PFKFB3, raising the possibility that PFKFB3 up-regulation in this context is modulated through post-transcriptional mechanisms. Notably, we have found that the 3'-untranslated region of the PFKFB3 mRNA contains a combinatorial arrangement of a specific cis-acting element named cytoplasmic polyadenylation element (CPE) (Figure 5D).[25,26] CPEs are U-rich sequences that recruit the CPE-binding proteins (CPEB) that in turn promote cytoplasmic poly-adenylation and translational activation.[26–35] Therefore, we postulated that CPEB4-mediated translation could be required to increase PFKFB3 protein expression and activate HSCs. In support of this possibility, we found that CPEB4 protein expression was increased in both human LX2 cells (Figure 5E) and in primary mouse HSCs (Figure 5F), correlating with PFKFB3 overexpression and HSC activation (Figure 3C), as demonstrated by immunoblotting and co-immunofluorescence. CPEB4 up-regulation was linked to the glycolytic status of HSCs. Thus, when the PFKFB3-dependent glycolysis of HSCs was inhibited by 3PO, the overexpression of CPEB4 was attenuated (Figures 5G and H), suggesting that a molecular circuit composed of CPEB4 and PFKFB3 controls glycolytic reprogramming in HSCs.

The RNA Binding Protein CPEB4 Post-Transcriptionally Regulates PFKFB3 Expression and Induces an Activated Fibrogenic Phenotype in Hepatic Stellate Cells

To better define the connection between CPEB4 function and PFKFB3, we performed RNA-protein co-immunopre-cipitation studies in LX2 cells (Figure 6A). An antibody targeting our RNA-binding protein of interest was used to immunoprecipitate CPEB4 and any interacting molecules from the HSC lysates. Reverse transcription followed by polymerase reaction was then used to identify individual PFKFB3 mRNAs isolated with CPEB4. This is a reliable tool to study the interaction of CPEB4 to the target PFKFB3 mRNA in HSCs. We found that PFKFB3 transcripts were enriched in the CPEB4 co-immunoprecipitation compared to the IgG co-immunoprecipitation (Figure 6B), demonstrating that PFKFB3 mRNA is indeed a direct target of CPEB4 in activated HSCs. To corroborate our findings, we used

Figure 3. PFKFB3 protein expression is elevated in fibrotic human and rodent livers. (A) PFKFB3 immunoblotting and protein expression quantification in human healthy human liver and hepatitis C virus–related cirrhotic liver. (B) PFKFB3 immuno-staining in cirrhotic human liver sections, showing PFKFB3-positive spindle cells in fibrous septa (arrowheads). Scale bars: 100 μm (left), 50 μm (middle), 25 μm (right). (C) Immunoblotting and protein expression quantification for PFKFB3 and αSMA in rat liver at different time points after BDL, and in sham-operated control rats. Total, cytosolic, and nuclear fractions were studied. Two major PFKFB3 immunoreactive bands were detected, which may represent post-translational modifications. (D) Immunoblotting and protein expression quantification for the indicated proteins in mouse liver at different time points after BDL and in sham mice. (E) Co-immunofluorescence showing spindle cells (arrowheads) co-expressing PFKFB3 (red), and αSMA (green) in portal tracts of BDL mice. 4,6-diamidino-2-phenylindole–stained nuclei (blue). Scale bar: 50 μm (F) PFKFB3 immunohis-tochemistry in portal tracts of BDL mouse liver. Scale bar: 50 μm (G) Ki67 immunohistochemistry in portal tracts of BDL mouse liver. Scale bar: 25 μm. *P < .05; **P < .01.
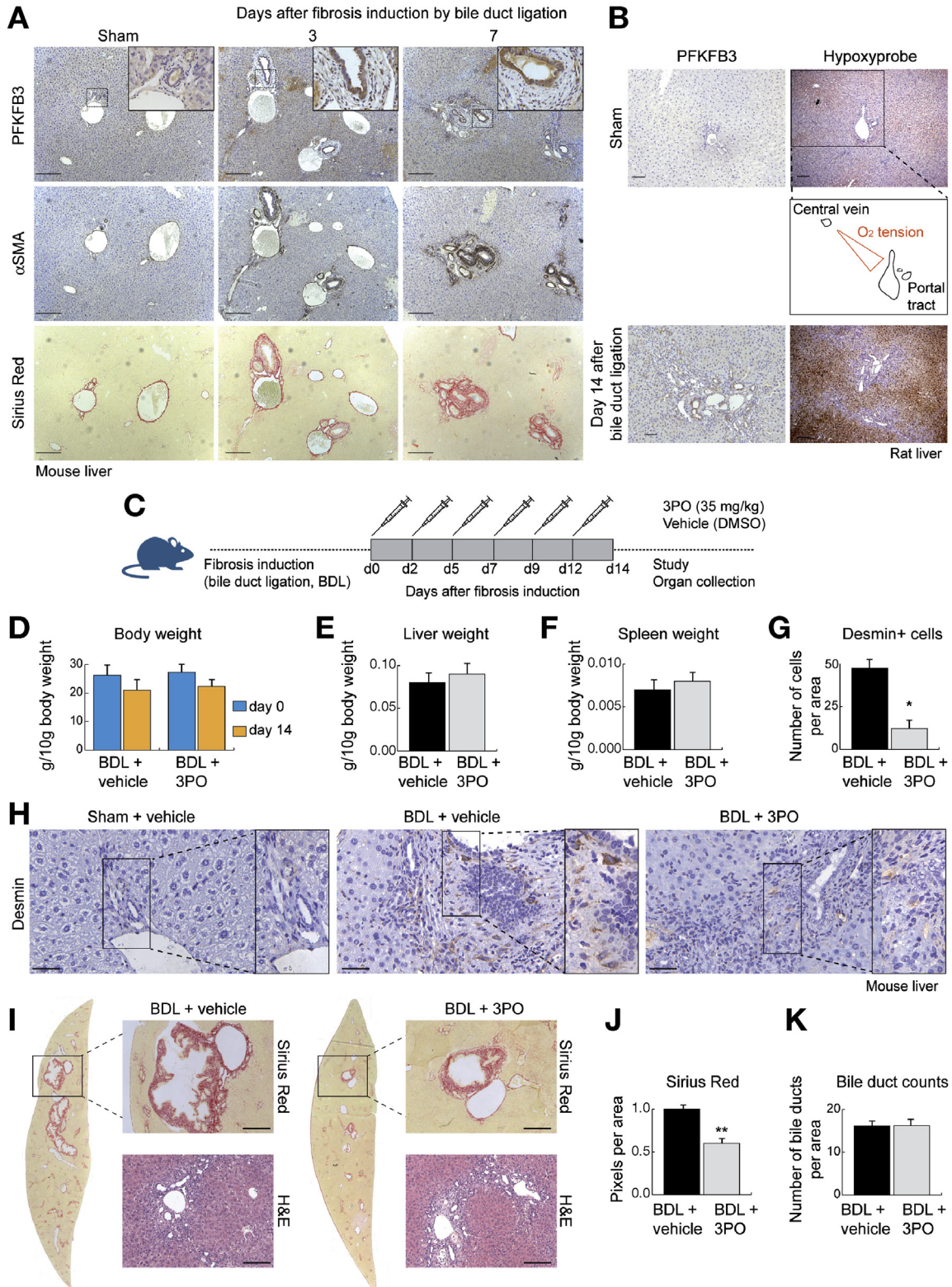
Figure 4. PFKFB3 blockade attenuates liver fibrosis in vivo. (*A*) PFKFB3 immunohistochemistry (*top*), αSMA immunohisto-chemistry (*middle*), and Sirius Red histological staining (*bottom*) in serial liver sections from mice subjected to fibrosis induction by BDL, and from sham-operated control animals. Scale bar: 200 μm. (*B*) Comparison between PFKFB3 immunohistochemistry and hypoxyprobe immunohistostaining (hypoxic areas stained in *brown*) in the liver from sham or BDL rats. Scale bars: 100 μm (PFKFB3), 200 μm (hypoxyprobe). (*C*) Experimental set-up. (*D*) Body weight in BDL mice before and after treatment with 3PO or vehicle. (*E*) Liver weight in BDL mice treated with 3PO or vehicle. (*F*) Spleen weight. (*G*) Quantification of desmin-positive cells. (*H*) Desmin immunohistochemistry in the liver from BDL mice treated with 3PO or vehicle and in sham mice. Scale bar: 100 μm. (*I*) Sirius Red staining and H&E staining in BDL mouse liver after 3PO or vehicle. Scale bar: 100 μm (Sirius Red), 200 μm (H&E). (*J*) Sirius Red quantification. *$P < .001$. (*K*) Quantification of bile ducts in BDL mice treated with 3PO or vehicle.
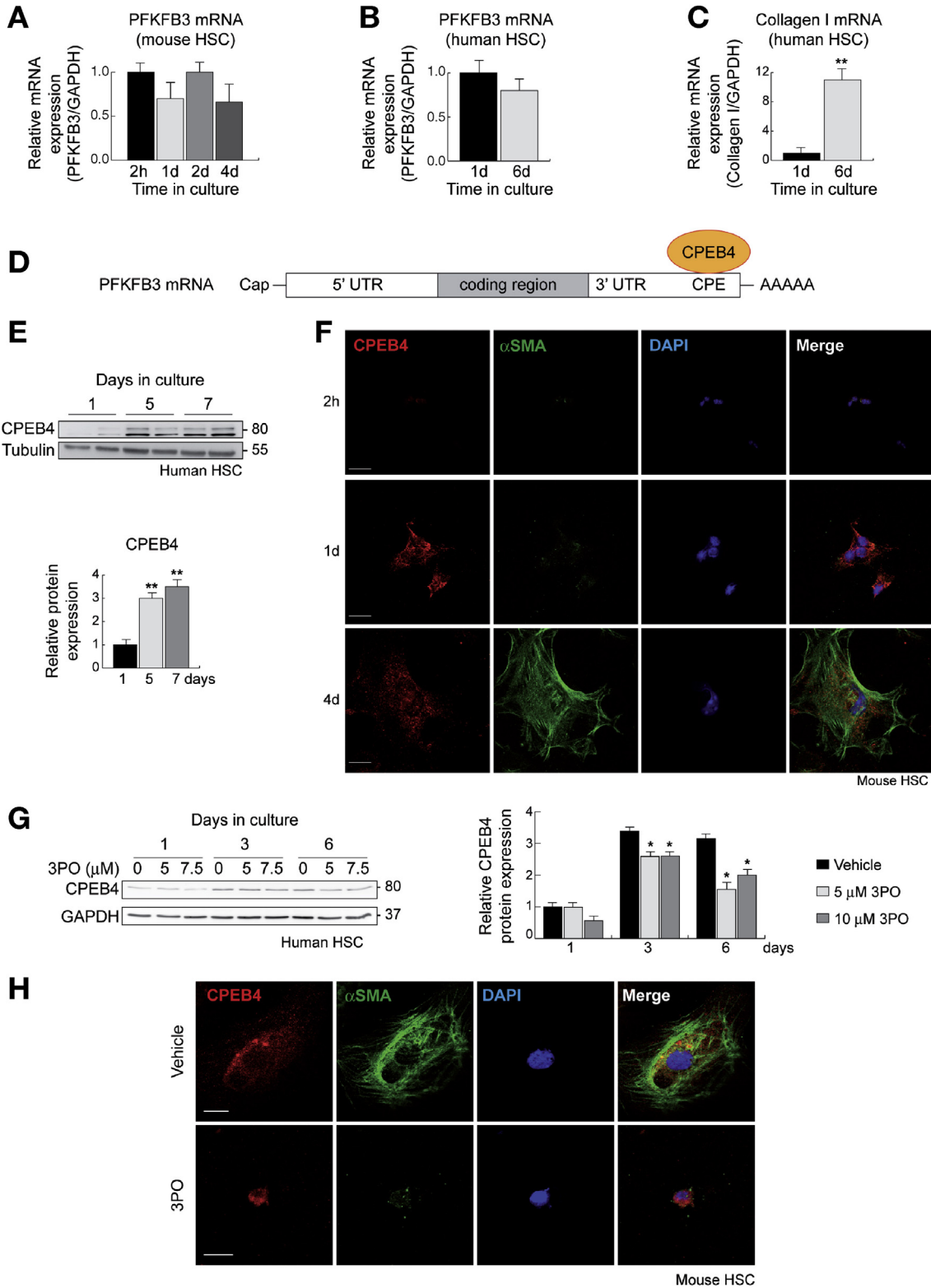
Figure 5. CPEB4 is functionally linked with PFKFB3 during HSC activation. (*A*) PFKFB3 mRNA expression in mouse HSCs. (*B*) PFKFB3 mRNA expression in LX2 cells. (*C*) Collagen I mRNA expression in LX2 cells. (*D*) Schematic representation of PFKFB3 mRNA showing CPE sequences binding CPEB4 in 3'-untranslated region. (*E*) CPEB4 immunoblotting and protein expression quantification in LX2 cells. (*F*) Co-immunofluorescence for CPEB4 (*red*) and αSMA (*green*) in mouse HSCs. 4,6-diamidino-2-phenylindole (DAPI)–stained nuclei (blue). Scale bar: 25 μm. (*G*) CPEB4 immunoblotting and protein expression quantification in control or 3PO-treated LX2 cells. Data are mean ± SEM of 2–3 different experiments. (*H*) Co-immunofluorescence for CPEB4 (*red*) and αSMA (*green*) in control or 3PO-treated mouse HSCs. DAPI-stained nuclei (*blue*). Scale bar: 25 μm. *$P < .05$; **$P < .01$.
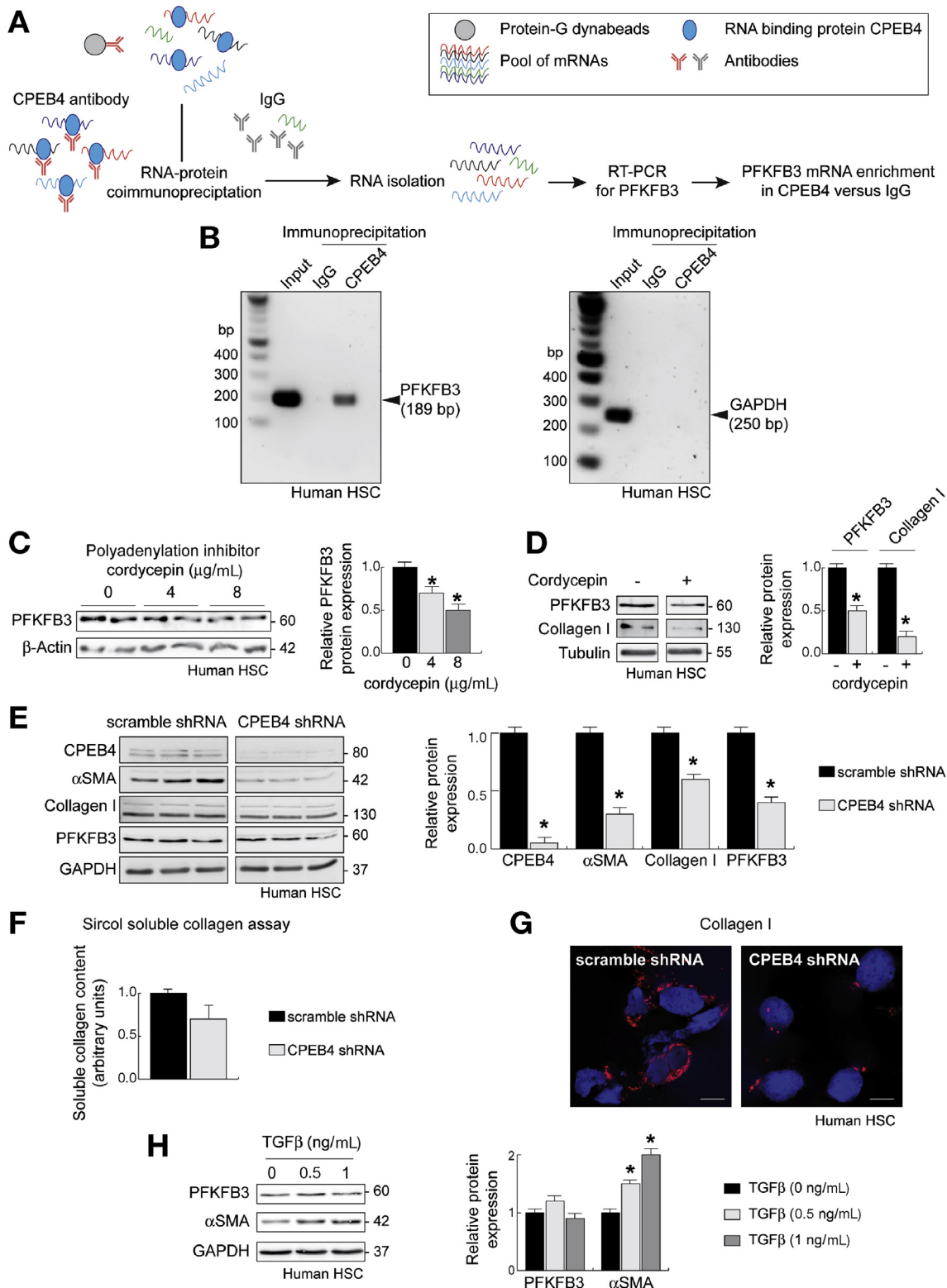
Figure 6. CPEB4 post-transcriptionally regulates PFKFB3 expression and induces an activated fibrogenic phenotype in HSCs. (*A*) Schematic diagram of RNA-protein immunoprecipitation method. (*B*) Reverse transcription polymerase chain reaction detection of PFKFB3 and glyceraldehyde 3-phosphate dehydrogenase mRNA levels after co-immunoprecipitation with CPEB4 in LX2 cells. (*C*) PFKFB3 immunoblotting and protein expression quantification in LX2 cells in presence or absence of the polyadenylation inhibitor cordycepin (4 and 8 μg/mL). (*D*) Immunoblotting and protein expression quantification for PFKFB3 and collagen I in LX2 cells in the presence or absence of cordycepin (4 μg/mL). Data are mean $\pm$ SEM of 2–3 different experiments. (*E*) Immunoblotting and protein expression quantification for the indicated proteins in LX2 cells transfected with scramble or CPEB4 shRNAs. (*F*) Soluble collagen content in LX2 transfected with scramble or CPEB4 shRNAs. (*G*) Collagen I immunofluorescence (*red*) in LX2 cells transfected with scramble or CPEB4 shRNAs. 4,6-diamidino-2-phenylindole–stained nuclei (blue). Scale bar: 25 μm. (*H*) Immunoblotting and protein expression quantification for PFKFB3 and αSMA in LX2 cells treated with TGFβ (0, 5, and 1 ng/mL) or vehicle. *$P < .05$.

BASIC AND
TRANSLATIONAL LIVER

cordycepin (3'-deoxyadenosine), a known inhibitor of CPEB-dependent polyadenylation.[25,36] Because of the 3'-deoxy moiety, this nucleoside analog acts by blocking poly(A) elongation. Pretreatment with cordycepin markedly disrupted the up-regulation of PFKFB3 observed in LX2 cells

(Figure 6C), leading to reduced collagen I protein expression (Figure 6D), indicating that polyadenylation is a critical process for PFKFB3 protein expression in activated HSCs.

To determine the functional impact of the regulation of PFKFB3 expression by CPEB4, we silenced CPEB4
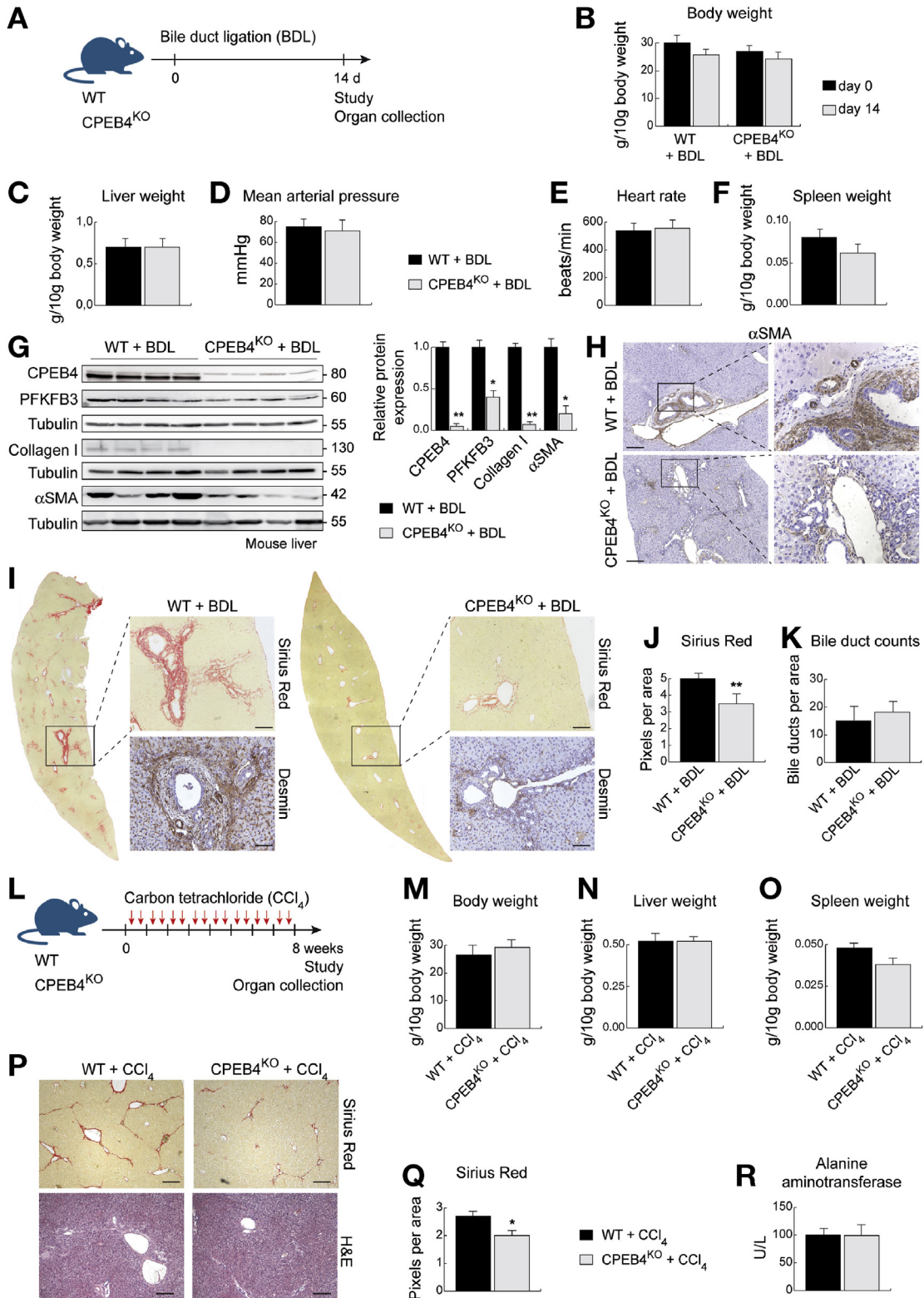
expression in LX2 cells using short hairpin RNAs (shRNAs). We transfected LX2 cells with recombinant lentiviruses expressing isopropylthio-β-galactoside–inducible shRNAs against CPEB4, and compared with LX2 cells expressing control shRNAs. Immunoblotting analysis of these cells demonstrated the robust and effective depletion of CPEB4 caused by CPEB4 shRNAs (Figure 6E), which attenuated PFKFB3 expression and, in turn, compromised the ability of HSCs to activate and produce extracellular matrix proteins, as demonstrated by the reduction in αSMA (Figure 6E; immunoblotting) and collagen I expression (Figure 6E–G; immunoblotting, Sircol soluble collagen assay, and immunofluorescence).

Because transforming growth factor–beta (TGFβ) promotes liver fibrosis by activating HSCs, and TGFβ transcriptionally up-regulates PFKFB3 mRNA in cancer cells,[37] we determined whether the profibrogenic effects of TGFβ involve PFKFB3 induction. Interestingly, we found that the dose-dependent activation of LX2 cells caused by TGFβ was not associated with a parallel increase in PFKFB3 expression (Figure 6H). This finding reinforces the idea that the mechanism mediating PFKFB3 protein up-regulation is cellular context–dependent, being, during HSC activation, mediated mainly by (CPEB4-driven) translational, and not transcriptional, reprogramming.

CPEB4 Deficiency in Knockout Mice Prevents PFKFB3 Up-Regulation and Fibrogenesis After Bile Duct Ligation and Carbon Tetrachloride Treatment

To complement the in vitro approach, we generated a global loss-of-function genetic mouse model (CPEB4^{KO}) to determine the effects of silencing CPEB4 expression in vivo on liver fibrogenesis. CPEB4^{KO} mice and their wild-type (WT) littermates were subjected to BDL to induce liver fibrosis and studied 14 days later (Figure 7A). CPEB4^{KO} BDL mice displayed no differences in body weight (Figure 7B), liver weight (Figure 7C), mean arterial pressure (Figure 7D), or heart rate (Figure 7E) compared with WT BDL controls. Spleen weight was decreased by 25% in CPEB4^{KO} BDL mice compared with WT BDL controls, but the difference was not statistically significant (Figure 7F). We demonstrated that CPEB4^{KO} mice have effective CPEB4 depletion in the liver (Figure 7G). This effect was accompanied by a significant decrease in PFKFB3 protein expression (Figure 7G), as found in CPEB4 knockdown HSCs (Figure 6E). These results

demonstrate that PFKFB3 levels are maintained high during liver fibrosis, owing to CPEB4-dependent translation. Interestingly, CPEB4^{KO} mice developed less-severe forms of fibrogenesis after BDL compared with WT animals, as demonstrated by immunoblotting of fibrillar collagen I (Figure 7G), αSMA immunoblotting and immunohistochemistry (Figure 7G and 7H), desmin immunohistochemistry (Figure 7I), and Sirius Red histologic staining (Figure 7I and J). Similar to that observed after inhibition of PFKFB3 enzymatic activity, the number of bile ducts was not affected by depletion of CPEB4 (Figure 7K), suggesting that the attenuation of liver fibrosis observed upon CPEB4 silencing was not mediated by interference with a potential profibrogenic function of biliary epithelial cells.

To further verify that the circuit CPEB4-PFKFB3 activates fibrogenesis in an HSC-preferential manner, we induced liver fibrosis in CPEB4^{KO} and WT mice by carbon tetrachloride (CCl$_4$) (0.5 μL/g body weight; intraperitoneal injections, 2 times per week for 8 weeks), thus reducing the ductular proliferation component (Figure 7L). We found no changes in body weight (Figure 7M) and liver weight (Figure 7N) comparing CCl$_4$-treated CPEB4^{KO} and WT mice. Spleen weight was 20% lower in CCl$_4$-treated CPEB4^{KO} mice than in WT controls (Figure 7O), but the difference did not reach statistical significance. Notably, depletion of CPEB4 significantly reduced fibrogenesis in the CCl$_4$-treated mice (Figures 7P and Q), compared with CCl$_4$-treated WT animals. Serum levels of alanine aminotransferase (a transaminase enzyme used as a measure of hepatocyte injury) were essentially unaltered in CCl$_4$-treated CPEB4^{KO} and WT control mice (Figure 7R), verifying that the lower liver fibrosis observed in CCl$_4$-treated CPEB4^{KO} was not a consequence of reduced hepatocellular damage induced by CCl$_4$. Collectively, these in vivo studies, together with the aforementioned in vitro studies, indicate that HSCs use the CPEB4-PFKFB3 axis to generate fibrosis. Obviously, hepatic fibrosis is a complex phenomenon orchestrated by a multitude of cells, mediators, and signaling pathways. It is important to note that, regardless of whether there is a single cell type (ie, HSCs) involved in the pharmacological action of 3PO or the CPEB4 targeting, or whether the effects are potentiated by a potential action on accessory profibrogenic cell types (ie, biliary cells), the net effect is a marked decrease in fibrosis. This is a highly relevant finding from a therapeutic and translational point of view, considering that there is an urgent need to develop new antifibrotic strategies.

Figure 7. CPEB4 deficiency in knockout mice prevents PFKFB3 up-regulation and fibrogenesis after BDL and CCl$_4$ treatment. (A) CPEB4^{KO} and WT mice were subjected to BDL to induce liver fibrosis and studied 14 days later. (B) Body weight in WT and CPEB4^{KO} mice before and after BDL. (C) Liver weight in WT and CPEB4^{KO} BDL mice. (D) Mean arterial pressure. (E) Heart rate. (F) Spleen weight. (G) Immunoblotting and protein expression quantification for the indicated proteins in WT and CPEB4^{KO} BDL mice. (H) αSMA immunostaining in the liver from WT and CPEB4^{KO} BDL mice. Scale bar: 200 μm. (I) Sirius Red staining and desmin immunostaining in WT and CPEB4^{KO} BDL mice. Scale bar: 100 μm. (J) Sirius Red quantification in WT and CPEB4^{KO} BDL mice. (K) Bile duct quantification in WT and CPEB4^{KO} BDL mice. (L) CPEB4^{KO} and WT mice were treated with CCl$_4$ (0.5 μL/g body weight; intraperitoneal injections, twice a week for 8 weeks) to induce liver fibrosis. (M) Body weight in CCl$_4$-treated WT and CPEB4^{KO} mice. (N) Liver weight in CCl$_4$-treated WT and CPEB4^{KO} mice. (O) Spleen weight in CCl$_4$-treated WT and CPEB4^{KO} mice. (P) Sirius Red and H&E staining in CCl$_4$-treated WT and CPEB4^{KO} mice. Scale bar: 200 μm. (Q) Sirius Red quantification in CCl$_4$-treated WT and CPEB4^{KO} mice. (R) Serum alanine aminotransferase levels measured in CCl$_4$-treated WT and CPEB4^{KO} mice at 48 hours after the last CCl$_4$ injection. *$P < .05$; **$P < .01$.

Discussion

Results presented here provide new insights into the molecular mechanisms of liver fibrogenesis and arouse hope for developing more effective antifibrotic therapies. Thus, this work unveils a previously unrecognized post-transcriptional regulatory circuit in activated HSCs, comprising the critical glycolytic enzyme PFKFB3 and the RNA-binding protein CPEB4, which maintains HSCs in fibrotic livers with a higher glycolytic activity than normal HSCs in healthy livers. This abnormal glycolytic reprogramming predisposes HSCs to activation, myofibroblast transdifferentiation, cellular proliferation, and extracellular matrix production and accumulation, resulting in exponentation of liver fibrosis.

Our findings position PFKFB3-dependent glycolysis as a hallmark of HSC activation in liver fibrosis. PFKFB3 protein is overexpressed during HSC activation in vitro, both in human LX2 stellate cells and in freshly isolated mouse HSCs. The protein expression of PFKFB3 is also consistently elevated in vivo in the liver of cirrhotic patients, and in experimental models of fibrosis in rats and mice. This PFKFB3 up-regulation is a cardinal feature required to enhance glycolytic flux and induce an activated profibrogenic phenotype, because PFKFB3 blockade impaired these changes and reduced matrix production in vitro and in vivo. Consequently, PFKFB3 inhibition could be an attractive target for therapeutic inhibition of fibrogenesis. Notably, based on our studies and previous data by other groups,[11,12] dual targeting of glycolysis and glutaminolysis (which cooperatively control HSC function) may provide an innovative and promising antifibrotic strategy.

Our studies also decipher the regulatory mechanism behind the up-regulation of PFKFB3 in HSCs, through the function of the cytoplasmic polyadenylation element binding protein CPEB4. This RNA-binding protein is an exemplary key post-transcriptional regulator,[26–35] which is overexpressed in chronic liver disease and is of paramount importance for fine-tuning protein synthesis and pathological cellular phenotypes, as we demonstrated recently.[38–40] Our present studies showing that CPEB4 plays an important role in HSC activation and fibrogenesis significantly extend our previous reports and provide an additional node of interaction between CPEB-mediated post-transcriptional misregulation and liver disease. Both in human LX2 cells and primary mouse HSCs, we found that PFKFB3 protein overexpression was not accompanied by PFKFB3 mRNA up-regulation, indicating that it was not transcriptionally derived. Instead, we observed that PFKFB3 protein levels were maintained high during HSC transdifferentiation, owing to activation of cytoplasmic polyadenylation and translation by CPEB4. Thus, CPEB4 protein is up-regulated early during HSC activation and binds directly to CPE elements present on the 3'-untranslated region of the PFKFB3 transcript. This favors PFKFB3 mRNA cytoplasmic polyadenylation and, in turn, activates translation and generates high levels of the glycolysis activator PFKFB3. This mechanism does not exclude an additional regulation of PFKFB3 expression. Hence, it is not unusual for key proteins to be regulated at multiple levels, including transcription, translation, post-translational modifications, and/or protein degradation.[23,24,41] However, in the case of PFKFB3 and its regulation by CPEB4 in HSCs during liver injury, the translational regulation either precedes or dominates over transcriptional control, as activated HSCs in which CPEB4 has been silenced with shRNAs failed to up-regulate PFKFB3 to the levels observed in HSCs transfected with control shRNAs. In addition, CPEB4[KO] mice subjected to BDL were unable to up-regulate PFKFB3 expression to the levels observed in the fibrotic WT mice. Of note, silencing CPEB4 prevents the up-regulation of PFKFB3 observed in pathological conditions (ie, activated LX2 cells, bile duct–ligated mice), but does not completely abrogate PFKFB3 protein expression, which is necessary to maintain cellular homeostasis, suggesting the possible benefit of using CPEB4 inhibitors.

The sum of these findings puts the CPEB4-PFKFB3-dependent axis into the spotlight as a potential target for antifibrotic strategies. This is relevant because there is an urgent need for development of novel antifibrotic agents.[2,3] Of note, pharmacological PFKFB3 inhibitors such as 3PO are showing great promise as powerful therapies to target cancer,[42,43] and are already entering phase I clinical trials in patients with advanced malignancies.[44] Furthermore, antiglycolytic strategies employing PFKFB3 blockers have been shown to be particularly beneficial in different cell types because they only partially inhibit glycolysis (commonly by 40%–50%).[10,19] In our studies, 3PO at low doses reduced glycolysis by 51%, impairing HSC activation without causing HSC death in vitro. In addition, a partial and daily decrease of glycolysis sufficed to suppress pathological fibrogenesis in vivo in bile duct–ligated mice with acceptable tolerability. This is important because approaches that block glycolysis completely have been shown to cause adverse (toxic) effects.[10,19] The reason for the partial effect likely relates to the fact that 3PO blocks an activator of a key enzyme in glycolysis (PFK1), but has no direct effect on PFK1, which shares an identical substrate, fructose-6-phosphate.[10,18,19] Hence, PFKFB3 blockade has a ceiling level in its ability to inhibit glycolysis. Our data also provide proof-of-concept that targeting CPEB4 may be efficacious in treating liver fibrosis. Of note, we are currently developing different therapeutic approaches to selectively block the activities of CPEBs.[45,46] These may counteract fibrosis progression by obstructing the metabolic evolution of activated HSCs without causing damage to healthy cells, and are therefore an attractive new strategy in the battle against chronic liver disease. It is hoped that these CPEB4 inhibitors will make it to the clinic in the near future.

Supplementary Material

Note: To access the supplementary material accompanying this article, visit the online version of *Gastroenterology* at www.gastrojournal.org, and at http://dxdoi.org/10.1053/j.gastro.2020.03.008.

References

1. Schuppan D, Afdhal NH. Liver cirrhosis. Lancet 2008; 371:838–851.
2. Friedman SL. Evolving challenges in hepatic fibrosis. Nat Rev Gastroenterol Hepatol 2010;7:425–436.
3. Bataller R, Brenner DA. Liver fibrosis. J Clin Invest 2005; 115:209–218.
4. Friedman SL. Hepatic stellate cells: protean, multifunctional, and enigmatic cells of the liver. Physiol Rev 2008; 88:125–172.
5. Warburg O. On the origin of cancer cells. Science 1956; 123:309–314.
6. Gatenby RA, Gillies RJ. Why do cancers have high aerobic glycolysis? Nat Rev Cancer 2004;4:891–899.
7. Pavlova NN, Thompson CB. The emerging hallmarks of cancer metabolism. Cell Metab 2016;23:27–47.
8. Chang CH, Curtis JD, Maggi LB Jr, et al. Post-transcriptional control of T cell effector function by aerobic glycolysis. Cell 2013;153:1239–1251.
9. Bernard K, Logsdon NJ, Ravi S, et al. Metabolic reprogramming is required for myofibroblast contractility and differentiation. J Biol Chem 2015;290:25427–25438.
10. **De Bock K, Georgiadou M**, Schoors S, et al. Role of PFKFB3-driven glycolysis in vessel sprouting. Cell 2013; 154:651–663.
11. Chen Y, Choi SS, Michelotti GA, et al. Hedgehog controls hepatic stellate cell fate by regulating metabolism. Gastroenterology 2012;143:1319–1329.
12. Du K, Hyun J, Premont RT, et al. Hedgehog-YAP signaling pathway regulates glutaminolysis to control activation of hepatic stellate cells. Gastroenterology 2018;154:1465–1479.
13. **Atsumi T, Chesney J**, Metz C, et al. High expression of inducible 6-phosphofructo-2-kinase/fructose-2,6-bisphosphatase (iPFK-2; PFKFB3) in human cancers. Cancer Res 2002;62:5881–5887.
14. Van Schaftingen E, Jett MF, Hue L, et al. Control of liver 6-phosphofructokinase by fructose 2,6-bisphosphate and other effectors. Proc Natl Acad Sci U S A 1981; 78:3483–3486.
15. **Mederacke I, Dapito DH**, Affo S, et al. High-yield and high-purity isolation of hepatic stellate cells from normal and fibrotic mouse livers. Nat Protoc 2015;10:305–315.
16. Xu L, Hui AY, Albanis E, et al. Human hepatic stellate cell lines. LX-1 and LX-2: new tools for analysis of hepatic fibrosis. Gut 2005;54:142–151.
17. Van Schaftingen E, Lederer B, Bartrons R, et al. A kinetic study of pyrophosphate: fructose-6-phosphate phosphotransferase from potato tubers. Application to a microassay of fructose 2,6-bisphosphate. Eur J Biochem 1982;129:191–195.
18. Clem B, Telang S, Clem A, et al. Small-molecule inhibition of 6-phosphofructo-2-kinase activity suppresses glycolytic flux and tumor growth. Mol Cancer Ther 2008; 7:110–120.
19. **Schoors S, De Bock K, Cantelmo AR**, et al. Partial and transient reduction of glycolysis by PFKFB3 blockade reduces pathological angiogenesis. Cell Metab 2014; 19:37–48.
20. Vander Heiden MG, Cantley LC, Thompson CB. Understanding the Warburg effect: the metabolic requirements of cell proliferation. Science 2009;324:1029–1033.
21. DeBerardinis RJ, Lum JJ, Hatzivassiliou G, et al. The biology of cancer: metabolic reprogramming fuels cell growth and proliferation. Cell Metab 2008;7:11–20.
22. Yalcin A, Clem BF, Simmons A, et al. Nuclear targeting of 6-phosphofructo-2-kinase (PFKFB3) increases proliferation via cyclin-dependent kinases. J Biol Chem 2009; 284:24223–24232.
23. **Obach M, Navarro-Sabate A**, Caro J, et al. 6-Phosphofructo-2-kinase (pfkfb3) gene promoter contains hypoxia-inducible factor-1 binding sites necessary for transactivation in response to hypoxia. J Biol Chem 2004;279:53562–53570.
24. Rosmorduc O, Wendum D, Corpechot C, et al. Hepatocellular hypoxia-induced vascular endothelial growth factor expression and angiogenesis in experimental biliary cirrhosis. Am J Pathol 1999;155:1065–1073.
25. Domenech E, Maestre C, Esteban-Martinez L, et al. AMPK and PFKFB3 mediate glycolysis and survival in response to mitophagy during mitotic arrest. Nat Cell Biol 2015;17:1304–1316.
26. Pique M, Lopez JM, Foissac S, et al. A combinatorial code for CPE-mediated translational control. Cell 2008; 132:434–448.
27. Mendez R, Hake LE, Andresson T, et al. Phosphorylation of CPE binding factor by Eg2 regulates translation of c-mos mRNA. Nature 2000;404:302–307.
28. Groisman I, Huang YS, Mendez R, et al. CPEB, maskin, and cyclin B1 mRNA at the mitotic apparatus: implications for local translational control of cell division. Cell 2000;103:435–447.
29. Weill L, Belloc E, Bava FA, et al. Translational control by changes in poly(A) tail length: recycling mRNAs. Nat Struct Mol Biol 2012;19:577–585.
30. Weill L, Belloc E, Castellazzi CL, et al. Musashi 1 regulates the timing and extent of meiotic mRNA translational activation by promoting the use of specific CPEs. Nat Struct Mol Biol 2017;24:672–681.
31. Eliscovich C, Peset I, Vernos I, et al. Spindle localized CPE-mediated translation controls meiotic chromosome segregation. Nat Cell Biol 2008;10:858–865.
32. Parras A, Anta H, Santos-Galindo M, et al. Autism-like phenotype and risk gene mRNA deadenylation by CPEB4 mis-splicing. Nature 2018;560:441–446.
33. Ortiz-Zapater E, Pineda D, Martinez-Bosch N, et al. Regulation of gene expression during pancreatic cancer progression: a role for CPEB4. Nat Med 2012;18:83–90.
34. Novoa I, Gallego J, Ferreira PG, et al. Mitotic cell cycle progression is regulated by CPEB-dependent translational control. Nat Cell Biol 2010;12:447–456.
35. Bava FA, Eliscovich C, Ferreira PG, et al. CPEB1 coordinates alternative 3'UTR formation with translational regulation. Nature 2013;495:121–125.
36. Rose KM, Bell LE, Jacob ST. Specific inhibition of chromatin-associated poly(A) synthesis *in vitro* by cordycepin 5'-triphosphate. Nature 1977;267:178–180.
37. Rodriguez-Garcia A, Samso P, Fontova P, et al. TGF-β1 targets Smad, p38 MAPK, and PI3K/Akt signaling

pathways to induce PFKFB3 gene expression and glycolysis in glioblastoma cells. FEBS J 2017;284:3437–3454.

38. **Calderone V, Gallego J**, Fernandez-Miranda G, et al. Sequential functions of CPEB1 and CPEB4 regulate pathologic expression of VEGF and angiogenesis in chronic liver disease. Gastroenterology 2016;150:982–997.

39. Garcia-Pras E, Gallego J, Coch L, et al. Role and therapeutic potential of vascular stem/progenitor cells in pathological neovascularisation during chronic portal hypertension. Gut 2017;66:1306–1320.

40. Maillo C, Martin J, Sebastian D, et al. Circadian- and UPR-dependent control of CPEB4 mediates a translational response to counteract hepatic steatosis under ER stress. Nat Cell Biol 2017;19:94–105.

41. **Duran J, Obach M**, Navarro-Sabate A, et al. Pfkfb3 is transcriptionally upregulated in diabetic mouse liver through proliferative signals. FEBS J 2009;276:4555–4568.

42. **Clem BF, O'Neal J**, Tapolsky G, et al. Targeting 6-phosphofructo-2-kinase (PFKFB3) as a therapeutic strategy against cancer. Mol Cancer Ther 2013;12:1461–1470.

43. **Cantelmo AR, Conradi LC, Brajic A**, et al. Inhibition of the glycolytic activator PFKFB3 in endothelium induces tumor vessel normalization, impairs metastasis, and improves chemotherapy. Cancer Cell 2016;30:968–985.

44. Telang S, O'Neal J, Tapolsky G, et al. Discovery of a PFKFB3 inhibitor for phase I trial testing that synergizes with the B-Raf inhibitor vemurafenib. Cancer Metab 2014;2(Suppl 1):P14.

45. Afroz T, Skrisovska L, Belloc E, et al. A fly trap mechanism provides sequence-specific RNA recognition by CPEB proteins. Genes Dev 2014;28:1498–1514.

46. Villanueva E, Navarro P, Rovira-Rigau M, et al. Translational reprogramming in tumor cells can generate oncoselectivity in viral therapies. Nat Commun 2017; 8:14833.

Author names in bold designate shared co-first authorship.

Correspondence
Address correspondence to: Mercedes Fernandez, PhD, August Pi i Sunyer Biomedical Research Institute, Rossello 149-153, 08036 Barcelona, Spain. e-mail: mercefernandez@ub.edu.